Commun. Comput. Phys.
doi: 10.4208/cicp.100412.041112a

Vol. **14**, No. 3, pp. 621-638
September 2013

On the Construction of Well-Conditioned Hierarchical Bases for $\mathcal{H}(\mathbf{div})$-Conforming $\mathbb{R}^n$ Simplicial Elements

Jianguo Xin[1], Wei Cai[1,*] and Nailong Guo[2]

[1] *Department of Mathematics and Statistics, University of North Carolina at Charlotte, Charlotte, NC 28223, USA.*
[2] *Mathematics and Computer Science Department, Benedict College, Columbia, SC 29204, USA.*

Received 10 April 2012; Accepted (in revised version) 4 November 2012

Available online 25 January 2013

Abstract. Hierarchical bases of arbitrary order for $\mathcal{H}(\mathbf{div})$-conforming triangular and tetrahedral elements are constructed with the goal of improving the conditioning of the mass and stiffness matrices. For the basis with the triangular element, it is found numerically that the conditioning is acceptable up to the approximation of order four, and is better than a corresponding basis in the dissertation by Sabine Zaglmayr [High Order Finite Element Methods for Electromagnetic Field Computation, Johannes Kepler Universität, Linz, 2006]. The sparsity of the mass matrices from the newly constructed basis and from the one by Zaglmayr is similar for approximations up to order four. The stiffness matrix with the new basis is much sparser than that with the basis by Zaglmayr for approximations up to order four. For the tetrahedral element, it is identified numerically that the conditioning is acceptable only up to the approximation of order three. Compared with the newly constructed basis for the triangular element, the sparsity of the mass matrices from the basis for the tetrahedral element is relatively sparser.

AMS subject classifications: 65N30, 65F35, 65F15

Key words: Hierarchical bases, simplicial $\mathcal{H}(\mathbf{div})$-conforming elements, matrix conditioning.

1 Introduction

In this paper we are concerned with the construction of well-conditioned hierarchical bases of arbitrary order for $\mathcal{H}(\mathbf{div})$-conforming $\mathbb{R}^n$ simplicial elements. Such bases are useful with the mixed finite element method [1,2] for the second-order elliptic problems,

*Corresponding author. *Email address:* `wcai@uncc.edu` (W. Cai)

and may be applied with the conforming element for the numerical study of elasticity [3], electromagnetism [4], incompressible fluid flow [5], and magnetohydrodynamics [6].

In 1975 Raviart and Thomas [7] introduced the $\mathcal{H}(\mathbf{div})$-conforming triangular element for the mixed finite element method to solve the Poisson equation with zero Dirichlet boundary condition. Among other results, Nédélec [8] generalized the idea of Raviart and Thomas, and constructed the $\mathcal{H}(\mathbf{div})$-conforming tetrahedral element for the mixed finite element method, the so-called Nédélec element of the first kind. A totally different $\mathcal{H}(\mathbf{div})$-conforming tetrahedral element, the so-called Nédélec element of the second kind was constructed in 1986 [9]. Using different techniques Brezzi and collaborators [11] constructed two families of mixed finite elements for second order elliptic problems, including the $\mathcal{H}(\mathbf{div})$-conforming triangular element. Further generalization to three dimensions had been carried out in 1987 by Brezzi, *et al.* [12]. From the perspective of differential forms Hipmair [13] gave a canonical construction of the $\mathcal{H}(\mathbf{curl})$- and $\mathcal{H}(\mathbf{div})$-conforming $\mathbb{R}^n$ simplicial elements. See also the related works [14–17] from such a perspective. In addition to other results Ainsworth and Coyle [18] constructed hierarchical bases of arbitrary order for $\mathcal{H}(\mathbf{div})$-conforming tetrahedral element. With polynomial approximation of an odd-numbered degree, the issue with enforcing conformity arising from a hierarchical basis [19, 20] had also been addressed in [18]. For the $\mathcal{H}(\mathbf{div})$-conforming simplicial elements and using techniques different from those in [18] Zaglmayr [21] gave two sets of hierarchical bases of arbitrary order.

It is well known in the finite element community that a hierarchical basis is more suitable than a nodal basis for the p- and hp-adaptivity [22,23]. However, a critical issue with a hierarchical basis is that with a high-order approximation the conditioning of the mass and stiffness matrices becomes to worsen to the extent of rendering the approximation results questionable and even meaningless. The conditioning issue has been realized and addressed by various researchers in different context for several conforming approximations, for examples, in [24–30]. In this study we continue our previous efforts [28–30] and concentrate on constructing well-conditioned hierarchical bases for $\mathcal{H}(\mathbf{div})$-conforming simplicial elements. The conditioning issue with $\mathcal{H}(\mathbf{div})$-conforming simplicial elements has specifically never been dealt with in the studies [7–9, 11–13, 18, 21]. Nevertheless, this does not necessarily mean that the matrix conditioning is not an issue with a hierarchical basis for $\mathcal{H}(\mathbf{div})$-conforming simplicial elements. On the contrary, we show in this study that such an issue does exist, and the mass and stiffness matrices may become badly ill-conditioned with a high-order approximation, and that this issue is more pronounced with the three-dimensional $\mathcal{H}(\mathbf{div})$-conforming tetrahedral elements.

Our new construction is based upon the works [18,21] and is inspired by the research on orthogonal polynomials of several variables [31]. For the $\mathcal{H}(\mathbf{div})$-conforming tetrahedral elements and to achieve the goal of rendering the hierarchical basis well conditioned, our strategy is classifying shape functions into several groups, each of which is associated with a geometrical identity of the canonical reference tetrahedron [18], and making the shape functions orthonormal within each group with respect to the reference element. This is made possible by adroitly applying one fundamental result - Proposition 2.3.8

in the monograph [31]. Once we have the hierarchical basis for the three-dimensional tetrahedral elements, we use the strategy of *dimension reduction* to construct the basis for the two-dimensional triangular elements, and for this purpose we have combined part of the results obtained by Zaylmayr [21]. It is worthwhile to point out that in the construction of $\mathcal{H}(\mathbf{div})$-conforming tetrahedral elements Ainsworth and Coyle had applied Legendre polynomials, and for this peculiar choice it is found out that for the polynomial approximation of degree $p=2$, the twelve *edge-based face functions* are not linearly independent [18]. Thus, the hierarchical basis [18] for the $\mathcal{H}(\mathbf{div})$-conforming tetrahedral elements is not complete if the degree of polynomial approximation is greater than one. It should also be remarked that for a certain uniform polynomial approximation the hierarchical basis for $\mathcal{H}(\mathbf{div})$-conforming tetrahedral elements [21] is not complete either in the sense of the Nédélec element of the second kind [9] because the number of shape functions is less than the dimension of the polynomial approximation.

The rest of the paper is organized as follows. The construction of hierarchical basis functions for the $\mathcal{H}(\mathbf{div})$-conforming tetrahedral and triangular elements is given in Section 2 and Section 3, respectively, on the canonical reference element. For the construction of global basis functions, one can use the Piola transform [10]. Numerical results of matrix conditioning and sparsity are reported in Section 4. Discussion and concluding remarks are presented in Section 5.

2 Basis functions for $\mathcal{H}(\mathbf{div})$-conforming tetrahedral elements

The result in Proposition 2.3.8 can be found in the monograph [31] with some corrections given in [30]. We construct shape functions for the $\mathcal{H}(\mathbf{div})$-conforming tetrahedral element on the canonical reference 3-simplex. The shape functions are grouped into several categories based upon their geometrical entities on the reference 3-simplex [18]. The basis functions in each category are constructed so that they are orthonormal on the reference element.

Any point in the 3-simplex K^3 is uniquely located in terms of the local coordinate system (ξ,η,ζ). The vertexes are numbered as $\mathbf{v}_0(0,0,0),\mathbf{v}_1(1,0,0),\mathbf{v}_2(0,1,0),\mathbf{v}_3(0,0,1)$. The barycentric coordinates are given as

$$\lambda_0:=1-\xi-\eta-\zeta,\quad \lambda_1:=\xi,\quad \lambda_2:=\eta,\quad \lambda_3:=\zeta. \tag{2.1}$$

The directed tangent on a generic edge $\mathbf{e}_j=[j_1,j_2]$ is defined as

$$\tau^{\mathbf{e}_j}:=\tau^{[j_1,j_2]}=\mathbf{v}_{j_2}-\mathbf{v}_{j_1},\quad j_1<j_2. \tag{2.2}$$

The edge is parametrized as

$$\gamma_{\mathbf{e}_j}:=\lambda_{j_2}-\lambda_{j_1},\quad j_1<j_2. \tag{2.3}$$

A generic edge can be uniquely identified with

$$\mathbf{e}_j:=[j_1,j_2],\quad j_1=0,1,2,\quad j_1<j_2\le 3,\quad j=j_1+j_2+\mathrm{sgn}(j_1). \tag{2.4}$$

Each face on the 3-simplex can be identified by the associated three vertexes, and is uniquely defined as

$$\mathbf{f}_{j_1} := [j_2, j_3, j_4], \quad 0 \le \{j_1, j_2, j_3, j_4\} \le 3, \quad j_2 < j_3 < j_4. \tag{2.5}$$

The standard bases in $\mathbb{R}^n$ are noted as $\vec{e}_i$, $i = 1, \cdots, n$, and $n = \{2, 3\}$.

2.1 Face functions

The face functions are further grouped into two categories: edge-based face functions and face bubble functions.

Edge-based face functions

These functions are associated with the three edges of a certain face $\mathbf{f}_{j_1}$, and by construction all have non-zero normal components only on the associated face $\mathbf{f}_{j_1}$, *viz.*

$$\mathbf{n}^{\mathbf{f}_{j_k}} \cdot \Phi^{\mathbf{f}_{j_1}, i}_{\mathbf{e}[k_1, k_2]} = 0, \quad j_k \neq j_1, \tag{2.6}$$

where $\mathbf{n}^{\mathbf{f}_{j_k}}$ is the unit outward normal vector to face $\mathbf{f}_{j_k}$.

The orthonormal shape functions are given as

$$\Phi^{\mathbf{f}_{j_1}, i}_{\mathbf{e}[k_1, k_2]} = C_i \lambda_{k_3} (1 - \lambda_{k_1})^i P_i^{(3,0)} \left(\frac{2\lambda_{k_2}}{1 - \lambda_{k_1}} - 1 \right) \frac{\nabla \lambda_{k_1} \times \nabla \lambda_{k_2}}{|\nabla \lambda_{k_1} \times \nabla \lambda_{k_2}|}, \tag{2.7a}$$

where

$$C_i = \sqrt{3(2i+4)(2i+5)}, \quad i = 0, 1, \cdots, p-1, \tag{2.7b}$$

and

$$k_1 = \{j_2, j_3\}, \quad k_2 = \{j_3, j_4\}, \quad k_1 < k_2, \quad k_3 = \{j_2, j_3, j_4\} \setminus \{k_1, k_2\}. \tag{2.7c}$$

In the formula (2.7a), the function $P_i^{(3,0)}(\bullet)$ is the classical *un-normalized* Jacobi polynomial of degree i with a single variable [32]. One can prove the orthonormal property of these edge-based face functions

$$\left\langle \Phi^{\mathbf{f}_{j_1}, m}_{\mathbf{e}[k_1, k_2]}, \Phi^{\mathbf{f}_{j_1}, n}_{\mathbf{e}[k_1, k_2]} \right\rangle \Big|_{K^3} = \delta_{mn}, \quad \{m, n\} = 0, 1, \cdots, p-1, \tag{2.8}$$

where δ_{mn} is the Kronecker delta. Note that with our new construction, the edge-based face functions are all linearly independent, which is also verified by the fact that in the spectrum of the mass (Gram) matrix, none of the eigenvalues is zero. More details can be found in Section 4.

Face bubble functions

The face bubble functions which belong to each specific group are associated with a particular face $\mathbf{f}_{j_1}$. They vanish on all edges of the reference 3-simplex K^3, and the normal components of which vanish on other three faces, *viz.*

$$\mathbf{n}^{\mathbf{f}_{j_k}} \cdot \Phi_{m,n}^{\mathbf{f}_{j_1}} = 0, \quad j_k \neq j_1. \tag{2.9}$$

The explicit formula is given as

$$\begin{aligned}\Phi_{m,n}^{\mathbf{f}_{j_1}} = &\iota(1-\lambda_{j_2})^m(1-\lambda_{j_2}-\lambda_{j_3})^n P_m^{(2n+3,2)}\left(\frac{2\lambda_{j_3}}{1-\lambda_{j_2}}-1\right)\\ &\times P_n^{(0,2)}\left(\frac{2\lambda_{j_4}}{1-\lambda_{j_2}-\lambda_{j_3}}-1\right)\frac{\nabla\lambda_{j_3}\times\nabla\lambda_{j_4}}{|\nabla\lambda_{j_3}\times\nabla\lambda_{j_4}|},\end{aligned} \tag{2.10}$$

where

$$\iota = C_m^n \lambda_{j_2}\lambda_{j_3}\lambda_{j_4}, \tag{2.11}$$

where

$$C_m^n = \frac{\sqrt{(2n+3)(m+n+3)(m+2n+4)(m+2n+5)(2m+2n+7)(2m+2n+8)(2m+2n+9)}}{\sqrt{(m+1)(m+2)}}, \tag{2.12}$$

and

$$0 \le \{m,n\}, m+n \le p-3. \tag{2.13}$$

By construction the face bubble functions share again the orthonormal property on the reference 3-simplex K^3:

$$< \Phi_{m_1,n_1}^{\mathbf{f}_{j_1}}, \Phi_{m_2,n_2}^{\mathbf{f}_{j_1}} > |_{K^3} = \delta_{m_1m_2}\delta_{n_1n_2}, \quad 0 \le \{m_1,m_2,n_1,n_2\}, m_1+n_1, m_2+n_2 \le p-3. \tag{2.14}$$

2.2 Interior functions

The interior functions are classified into three categories: edge-based, face-based and bubble interior functions. By construction the normal component of each interior function vanishes on all faces of the reference 3-simplex K^3, *viz.*

$$\mathbf{n}^{\mathbf{f}_j} \cdot \Phi^{\mathbf{t}} = 0, \quad j = \{0,1,2,3\}. \tag{2.15}$$

Edge-based interior functions

The tangential component of each edge-based function does not vanish on the associated only edge $\mathbf{e}_k := [k_1,k_2]$ but vanishes all other five edges, *viz.*

$$\tau^{\mathbf{e}_j} \cdot \Phi_{\mathbf{e}[k_1,k_2]}^{\mathbf{t},i} = 0, \quad \mathbf{e}_j \neq \mathbf{e}_k, \tag{2.16}$$

where $\tau^{\mathbf{e}_j}$ is the directed tangent along the edge $\mathbf{e}_j:=[j_1,j_2]$. The shape functions are given as

$$\Phi^{\mathbf{t},i}_{\mathbf{e}[k_1,k_2]}=C_i\lambda_{k_1}\lambda_{k_2}(1-\lambda_{k_1})^i P_i^{(1,2)}\left(\frac{2\lambda_{k_2}}{1-\lambda_{k_1}}-1\right)\frac{\tau^{\mathbf{e}_k}}{|\tau^{\mathbf{e}_k}|}, \tag{2.17a}$$

where

$$C_i=(i+3)\sqrt{\frac{(2i+4)(2i+5)(2i+7)}{i+1}}, \quad i=0,1,\cdots,p-2. \tag{2.17b}$$

Again one can prove the orthonormal property of edge-based interior functions:

$$<\Phi^{\mathbf{t},m}_{\mathbf{e}[k_1,k_2]},\Phi^{\mathbf{t},n}_{\mathbf{e}[k_1,k_2]}>|_{K^3}=\delta_{mn}, \quad \{m,n\}=0,1,\cdots,p-2. \tag{2.18}$$

Face-based interior functions

These functions which are associated with a particular face $\mathbf{f}_{j_1}$ have non-zero tangential components on their associated face only, and have no contribution to the tangential components on all other three faces, *viz.*

$$\mathbf{n}^{\mathbf{f}_{j_k}}\times\Phi^{\mathbf{t},\mathbf{f}_{j_1}}_{m,n}=\mathbf{0}, \quad j_k\neq j_1. \tag{2.19}$$

Further each face-based interior function vanishes on all the edges of the 3-simplex K^3, *viz.*

$$\tau^{\mathbf{e}_k}\cdot\Phi^{\mathbf{t},\mathbf{f}_{j_1}}_{m,n}=0. \tag{2.20}$$

The formulas of these functions are given as

$$\Phi^{\mathbf{t},\mathbf{f}^1_{j_1}}_{m,n}=\iota(1-\lambda_{j_2})^m(1-\lambda_{j_2}-\lambda_{j_3})^n P_m^{(2n+3,2)}\left(\frac{2\lambda_{j_3}}{1-\lambda_{j_2}}-1\right)P_n^{(0,2)}\left(\frac{2\lambda_{j_4}}{1-\lambda_{j_2}-\lambda_{j_3}}-1\right)\frac{\tau^{[j_2,j_3]}}{|\tau^{[j_2,j_3]}|}, \tag{2.21a}$$

$$\Phi^{\mathbf{t},\mathbf{f}^2_{j_1}}_{m,n}=\iota(1-\lambda_{j_2})^m(1-\lambda_{j_2}-\lambda_{j_3})^n P_m^{(2n+3,2)}\left(\frac{2\lambda_{j_3}}{1-\lambda_{j_2}}-1\right)P_n^{(0,2)}\left(\frac{2\lambda_{j_4}}{1-\lambda_{j_2}-\lambda_{j_3}}-1\right)\frac{\tau^{[j_2,j_4]}}{|\tau^{[j_2,j_4]}|}, \tag{2.21b}$$

where ι is given in (2.11) and $0\le\{m,n\},m+n\le p-3$. The face-based interior functions enjoy the orthonormal property on the reference 3-simplex K^3:

$$<\Phi^{\mathbf{t},\mathbf{f}^i_{j_1}}_{m_1,n_1},\Phi^{\mathbf{t},\mathbf{f}^i_{j_1}}_{m_2,n_2}>|_{K^3}=\delta_{m_1m_2}\delta_{n_1n_2},i=\{1,2\},0\le\{m_1,m_2,n_1,n_2\},m_1+n_1,m_2+n_2\le p-3. \tag{2.22}$$

Interior bubble functions

The interior bubble functions vanish on the entire boundary ∂K^3 of the reference 3-simplex K^3. The formulas of these functions are given as

$$\begin{aligned}\Phi^{\mathbf{t},\vec{e}_i}_{\ell,m,n}=&\chi P_\ell^{(2m+2n+8,2)}(2\lambda_1-1)P_m^{(2n+5,2)}\left(\frac{2\lambda_2}{1-\lambda_1}-1\right)\\&\times P_n^{(2,2)}\left(\frac{2\lambda_3}{1-\lambda_1-\lambda_2}-1\right)\vec{e}_i, \quad i=1,2,3,\end{aligned} \tag{2.23a}$$

where

$$\chi = C_{\ell,m,n}\lambda_0\lambda_1\lambda_2\lambda_3(1-\lambda_1)^m(1-\lambda_1-\lambda_2)^n, \tag{2.23b}$$

with

$$C_{\ell,m,n} = C^1_{\ell,m,n}C^2_{\ell,m,n}, \tag{2.23c}$$

where

$$C^1_{\ell,m,n} = \sqrt{\frac{(\ell+2m+2n+9)(\ell+2m+2n+10)(2\ell+2m+2n+11)(m+2n+6)}{(\ell+1)(m+1)(n+1)}}, \tag{2.23d}$$

$$C^2_{\ell,m,n} = \sqrt{\frac{(m+2n+7)(2m+2n+8)(n+3)(n+4)(2n+5)}{(\ell+2)(m+2)(n+2)}}, \tag{2.23e}$$

and

$$0 \le \{\ell,m,n\}, \ell+m+n \le p-4. \tag{2.23f}$$

Again, one can show the orthonormal property of the interior bubble functions

$$< \Phi^{\mathbf{t},\vec{e}_i}_{\ell_1,m_1,n_1}, \Phi^{\mathbf{t},\vec{e}_j}_{\ell_2,m_2,n_2} > |_{K^3} = \delta_{\ell_1\ell_2}\delta_{m_1m_2}\delta_{n_1n_2}, \tag{2.24a}$$

where

$$0 \le \{\ell_1,\ell_2,m_1,m_2,n_1,n_2\}, \ell_1+m_1+n_1, \ell_2+m_2+n_2 \le p-4, \quad \{i,j\} = 1,2,3. \tag{2.24b}$$

Following the same manner as in [18], it can be shown that the newly constructed basis is indeed a hierarchical one for $\mathcal{H}(\mathbf{div})$-conforming tetrahedral elements.

3 Basis functions for $\mathcal{H}(\mathbf{div})$-conforming triangular elements

Any point in the 2-simplex K^2 is uniquely located in terms of the local coordinate system (ξ,η). The vertexes are numbered as $\mathbf{v}_0(0,0), \mathbf{v}_1(1,0), \mathbf{v}_2(0,1)$. The barycentric coordinates are given as

$$\lambda_0 := 1-\xi-\eta, \quad \lambda_1 := \xi, \quad \lambda_2 := \eta. \tag{3.1}$$

The directed tangent on a generic edge $\mathbf{e}_j = [j_1,j_2]$ is similarly defined as in (2.2). The edge is also parametrized as in (2.3). A generic edge can be uniquely identified with

$$\mathbf{e}_j := [j_1,j_2], \quad j_1 = \{0,1\}, \quad j_1 < j_2 \le 2, \quad j = j_1+j_2. \tag{3.2}$$

The two-dimensional vectorial curl operator of a scalar quantity, which is used in our construction, needs a proper definition. We use the one given in the book [33], *viz.*

$$\mathbf{curl}(u) := \nabla \times u := \left[\frac{\partial u}{\partial \eta}, -\frac{\partial u}{\partial \xi}.\right]^\tau \tag{3.3}$$

Based upon the newly created shape functions for the three-dimensional $\mathcal{H}(\mathbf{div})$-conforming tetrahedral elements and using the technique of *dimension reduction* we construct the basis for the $\mathcal{H}(\mathbf{div})$-conforming triangular elements in two dimensions. However, it is easy to see that the two groups for the face functions cannot be appropriately modified for our purpose. Instead we borrow the idea of Zaglmayr in the dissertation [21], *viz.*, we combine the edge-based shape functions in [21] with our newly constructed edge-based and bubble interior functions. In [21] Zaglmayr had applied the so-called scaled integrated Legendre polynomials in the construction, *viz.*

$$\mathcal{L}_n^s(x,t) := t^{n-1}\int_{-t}^{x} \ell_{n-1}\left(\frac{\xi}{t}\right) d\xi, \quad n\geq 2, \quad t\in(0,1], \tag{3.4}$$

where $\ell_n(\bullet)$ is the classical un-normalized Legendre polynomial of degree n.

3.1 Edge functions

For the completeness of our basis construction, in this subsection we record the results in [21]. Associated with each edge the formulas for these functions are given as

$$\Phi^{N_0}_{\mathbf{e}[k_1,k_2]} = \lambda_{k_2}\nabla\times\lambda_{k_1} - \lambda_{k_1}\nabla\times\lambda_{k_2} \tag{3.5a}$$

for the lowest-order approximation and

$$\Phi^{j}_{\mathbf{e}[k_1,k_2]} = \nabla\times\left(\mathcal{L}^s_{j+2}(\gamma_{\mathbf{e}_k},\lambda_{k_2}+\lambda_{k_1})\right), \quad j=0,\cdots,p-1 \tag{3.5b}$$

for higher-order approximations.

3.2 Interior functions

The interior functions are further classified into two categories: edge-based and bubble interior functions. By construction the normal component of each interior function vanishes on either edge of the reference 2-simplex K^2, *viz.*

$$\mathbf{n}^{\mathbf{e}_j}\cdot\Phi^{\mathbf{t}} = 0, \quad j=\{1,2,3\}, \tag{3.6}$$

where $\mathbf{n}^{\mathbf{e}_j}$ is the unit outward normal vector to edge $\mathbf{e}_j$.

Edge-based interior functions

The tangential component of each edge-based function does not vanish on the associated only edge $\mathbf{e}_k := [k_1,k_2]$ but vanishes the other two edges, *viz.*

$$\tau^{\mathbf{e}_j}\cdot\Phi^{\mathbf{t},i}_{\mathbf{e}[k_1,k_2]} = 0, \quad \mathbf{e}_j\neq\mathbf{e}_k, \tag{3.7}$$

where $\tau^{\mathbf{e}_j}$ is the directed tangent along the edge $\mathbf{e}_j := [j_1, j_2]$. The shape functions are given as

$$\Phi^{\mathbf{t},i}_{\mathbf{e}[k_1,k_2]} = C_i \lambda_{k_1} \lambda_{k_2} (1-\lambda_{k_1})^i P_i^{(0,2)} \left(\frac{2\lambda_{k_2}}{1-\lambda_{k_1}} - 1 \right) \frac{\tau^{\mathbf{e}_k}}{|\tau^{\mathbf{e}_k}|}, \tag{3.8a}$$

where

$$C_i = \sqrt{2(i+2)(i+3)(2i+3)(2i+5)}, \quad i = 0,1,\cdots,p-2. \tag{3.8b}$$

The following orthonormal property of edge-based interior functions can be proved

$$< \Phi^{\mathbf{t},m}_{\mathbf{e}[k_1,k_2]}, \Phi^{\mathbf{t},n}_{\mathbf{e}[k_1,k_2]} > |_{K^2} = \delta_{mn}, \quad \{m,n\} = 0,1,\cdots,p-2. \tag{3.9}$$

Interior bubble functions

The interior bubble functions vanish on the entire boundary ∂K^2 of the reference 2-simplex K^2. The formulas of these functions are given as

$$\Phi^{\mathbf{t},\vec{e}_i}_{m,n} = C_{m,n} \lambda_0 \lambda_1 \lambda_2 (1-\lambda_0)^m P_m^{(2,2)} \left(\frac{\lambda_1 - \lambda_2}{1-\lambda_0} \right) P_n^{(2m+5,2)} (2\lambda_0 - 1) \vec{e}_i, \quad i = 1,2, \tag{3.10a}$$

where

$$C_{m,n} = \sqrt{\frac{(m+3)(m+4)(2m+5)(2m+n+6)(2m+n+7)(2m+2n+8)}{(m+1)(m+2)(n+1)(n+2)}}, \tag{3.10b}$$

and

$$0 \le \{m,n\}, m+n \le p-3. \tag{3.10c}$$

One can again prove the orthonormal property of the interior bubble functions

$$< \Phi^{\mathbf{t},\vec{e}_i}_{m_1,n_1}, \Phi^{\mathbf{t},\vec{e}_j}_{m_2,n_2} > |_{K^2} = \delta_{m_1 m_2} \delta_{n_1 n_2}, \tag{3.11a}$$

where

$$0 \le \{m_1, m_2, n_1, n_2\}, m_1 + n_1, m_2 + n_2 \le p-3, \quad \{i,j\} = 1,2. \tag{3.11b}$$

In a similar fashion as in [18], it can be shown that the newly constructed shape functions indeed form a hierarchical basis with polynomial approximation of degree p for $\mathcal{H}(\mathbf{div})$-conforming triangular elements.

4 Conditioning and sparsity of matrices

We check the conditioning of the mass matrix M and the stiffness matrix K on the reference element. With the mixed finite element method [1,2,7] the mass matrix comes from the variational formulation of the Laplacian in a second-order elliptic problem, e.g., the Poisson's equation in potential theory [34]

$$-\nabla\cdot\nabla u(\mathbf{x})=f(\mathbf{x}),\quad \mathbf{x}\in\Omega, \tag{4.1a}$$
$$u(\mathbf{x})=0,\qquad\qquad \mathbf{x}\in\partial\Omega. \tag{4.1b}$$

The weak formulation of this problem is that finding a pair of functions $(\mathbf{p},u)\in\mathcal{H}(\mathbf{div};\mathbf{\Omega})\times\mathcal{L}^2(\Omega)$ so that the following holds

$$\int_\Omega \mathbf{p}\cdot\mathbf{q}d\mathbf{x}+\int_\Omega u\nabla\cdot\mathbf{q}d\mathbf{x}=0,\quad \forall\mathbf{q}\in\mathcal{H}(\mathbf{div};\mathbf{\Omega}), \tag{4.2a}$$
$$\int_\Omega v(\nabla\cdot\mathbf{p}+f)d\mathbf{x}=0,\qquad \forall v\in\mathcal{L}^2(\Omega). \tag{4.2b}$$

The components of the mass matrix are defined as

$$M_{\ell_1,\ell_2}:=<\Phi_{\ell_1},\Phi_{\ell_2}>|_{K^d},\quad d=2,3. \tag{4.3}$$

The mass matrix M is symmetric and positive definite, and therefore has real positive eigenvalues. The condition number of a real symmetric positive definite matrix A is calculated by the formula

$$\kappa(A)=\frac{\lambda_{\max}}{\lambda_{\min}}, \tag{4.4}$$

where $\lambda_{\max}$ and $\lambda_{\min}$ are the maximum and minimum eigenvalues of the matrix A, respectively. For the incompressible fluid flows, e.g., governed by the Navier-Stokes equations [35] or by the magnetohydrodynamics equations [36] the authors [35,36] have applied the mixed finite element for the spatial discretization. In particular, they [35, 36] have used the $\mathcal{H}(\mathbf{div})$-conforming element for the Laplacian $\Delta\mathbf{u}$ of the velocity $\mathbf{u}$. In this case, we have the stiffness matrix K, which is defined component-wise as

$$K_{\ell_1,\ell_2}:=<\nabla\Phi_{\ell_1}:\nabla\Phi_{\ell_2}>|_{K^d},\quad d=2,3. \tag{4.5}$$

The stiffness matrix K is symmetric and semi-positive definite, and therefore has real non-negative eigenvalues. The condition number of the stiffness matrix K is calculated by the formula (4.4) with the zero eigenvalue excluded. We also check the sparsity of both matrices. Sparsity of a matrix affects directly the storage of the matrix in a computer.

4.1 The case with $\mathcal{H}(\mathbf{div})$-conforming tetrahedral elements

As we have pointed out in the introduction that neither the hierarchical basis by Ainsworth and Coyle [18] nor the one by Zaglmayr [21] spans the *complete* space of polynomial approximation of degree p, thus, we make no comparative study with these two bases, *viz.* only presenting the results from our newly constructed basis.

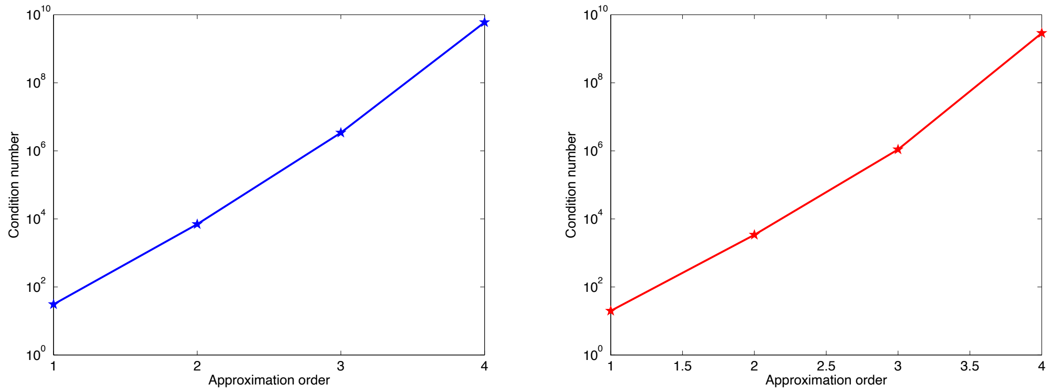

Figure 1: Condition number of the mass matrix (left) and stiffness matrix (right) for $\mathcal{H}(\mathbf{div})$-conforming tetrahedral elements.

For the polynomial approximations $p=\{1,2,3,4\}$, the condition numbers of the mass matrix are $\kappa(M_p)=\{3.08356e1,6.98681e3,3.41186e6,5.97230e9\}$. And for the stiffness matrix, they are $\kappa(K_p)=\{1.98918e1,3.39454e3,1.09441e6,2.88294e9\}$. So for each order of approximation, one can see that the condition numbers of the mass and stiffness matrix are on the same order. As the approximation order increases, the growth trend of the condition numbers is shown in Fig. 1. Up to third-order approximation and on the logarithmic scale, the condition numbers $\kappa(M_p)$ and $\kappa(K_p)$ grow about linearly with respect to the approximation order p. Starting from the order $p=4$, it diverges from linear growth. Since the condition numbers $\kappa(M_4)$ and $\kappa(K_4)$ are already large and on the order nine, *i.e.* $\mathcal{O}(10^9)$, from the practical point of view it is suggested that the newly derived hierarchical bases be applied up to order three.

The sparsity of the mass and stiffness matrices for the approximation order $p=\{1,2,3\}$ is shown in Figs. 2-4. For the mass matrix and for the approximation order $p=1$, there are 96 nonzero entries out of 144, accounting 66.67%; and for $p=2$, 444 out of 900, accounting 49.33%; and for $p=3$, 1550 out of 3600, accounting 43.06%. So the mass matrix M_p is relatively sparser as the approximation order p increases. For the stiffness matrix and for the approximation order $p=1$, there are 60 nonzero entries out of 144, accounting 41.67%; and for $p=2$, 528 out of 900, accounting 58.67%; and for $p=3$, 2046 out of 3600, accounting 56.83%.

4.2 The case with $\mathcal{H}(\mathbf{div})$-conforming triangular elements

Since we have borrowed the idea of Zaglmayr [21] for the construction of edge functions, regarding the performance of the newly constructed basis we make a comparative study with the one by Zaglmayr [21].

For the polynomial approximations $p=\{1,2,3,4\}$ and with the new basis, the condition numbers of the mass matrix are $\kappa(M_p^N)=\{2.01619e1,8.80420e1,9.84694e2,1.28619e4\}$ versus $\kappa(M_p^Z)=\{2.01619e1,8.40179e2,4.12583e3,1.59113e4\}$ for the basis by Zaglmayr [21].

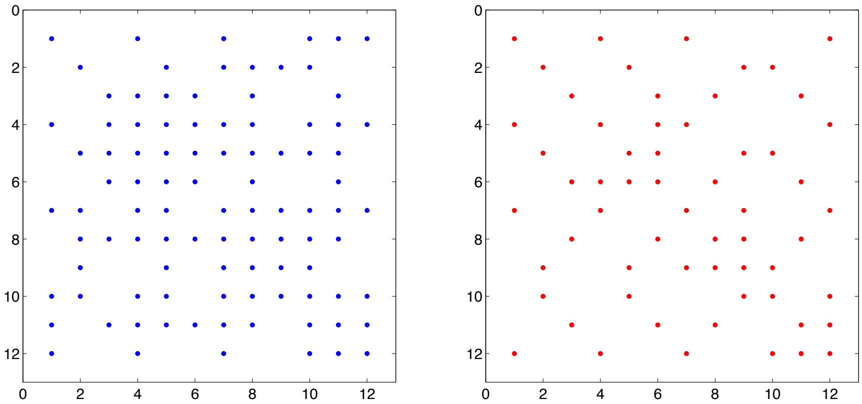

Figure 2: Sparsity of the mass matrix M_{p_1} (left) and stiffness matrix K_{p_1} (right) for $\mathcal{H}(\mathbf{div})$-conforming tetrahedral elements.

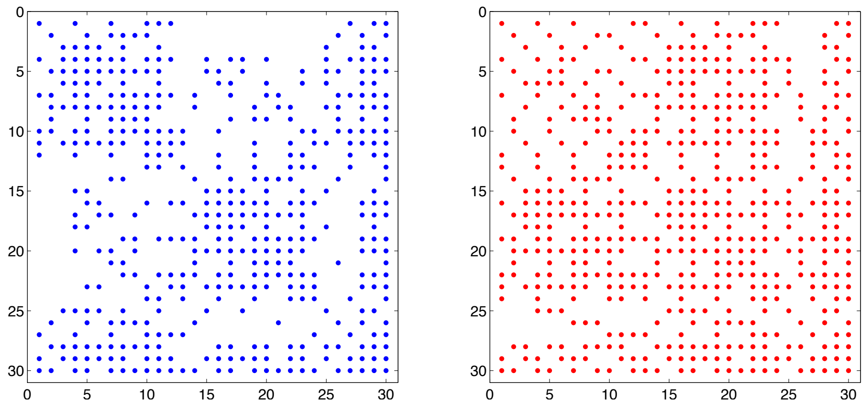

Figure 3: Sparsity of the mass matrix M_{p_2} (left) and stiffness matrix K_{p_2} (right) for $\mathcal{H}(\mathbf{div})$-conforming tetrahedral elements.

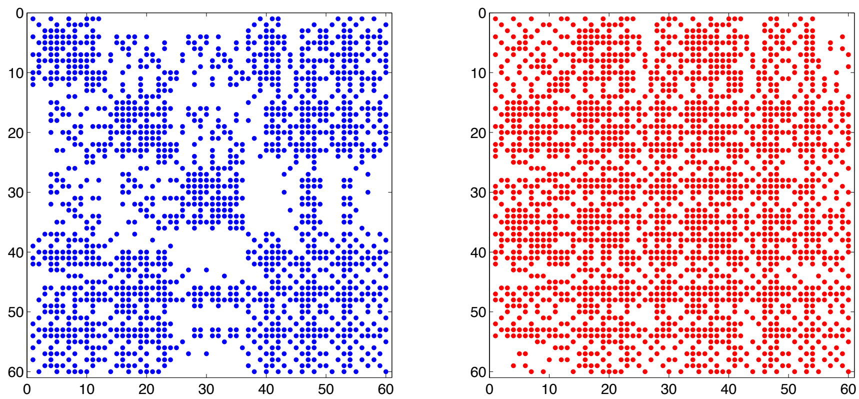

Figure 4: Sparsity of the mass matrix M_{p_3} (left) and stiffness matrix K_{p_3} (right) for $\mathcal{H}(\mathbf{div})$-conforming tetrahedral elements.

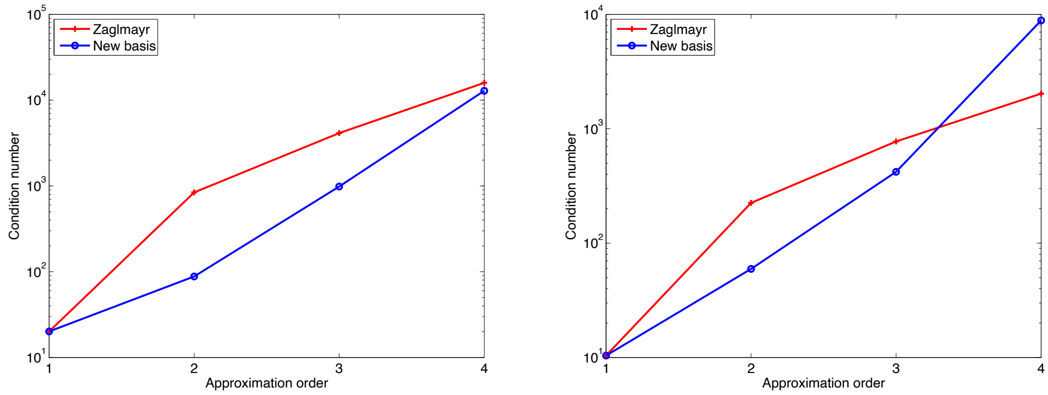

Figure 5: Condition number of the mass matrix (left) and stiffness matrix (right) for $\mathcal{H}(\mathbf{div})$-conforming triangular elements.

A significant difference is for the second- and third-order approximation: the conditioning has been improved about nine-fold and fourfold, respectively. The condition numbers of the stiffness matrix are $\kappa(K_p^N)=\{1.04039e1,5.95907e1,4.19692e2,8.84348e3\}$ for the new basis versus $\kappa(K_p^Z)=\{1.04039e1,2.24781e2,7.73521e2,2.02725e3\}$ for the basis by Zaglmayr [21]. The conditioning of the stiffness matrix for the second-order approximation has been improved about fourfold with the new basis. For each order of approximation and for both bases, the condition number of the mass matrix is greater than that of the stiffness matrix. With the increase of the approximation order, the growth trend of the condition numbers is shown in Fig. 5 for both matrices. As the condition number $\kappa(M_4)$ has already grown to the order four, *i.e.* $\mathcal{O}(10^4)$ for both bases, for practical applications, it is advised that the newly derived hierarchical bases be applied up to order four.

The comparison for the sparsity of mass matrices is shown in Figs. 6-8. For the approximation order $p=2$ and for the new basis and the one by Zaglmayr [21], there are 122 versus 116 nonzero entries out of 144, accounting 84.72% versus 80.56%; and for $p=3$, 290 versus 292 out of 400, accounting 72.50% versus 73.00%; and for $p=4$, 582 versus 600 out of 900, accounting 64.67% versus 66.67%. Thus, the mass matrix M_p is relatively sparser as the approximation order p increases for both bases. From Figs. 6-8 it can be seen that for each order of approximation, the pattern of sparsity for the mass matrix is somehow different. However, the percentage of sparsity, *i.e.* the ratio between the number of zero entries and the number of the full matrix is about the same for both bases.

The comparison for the sparsity of stiffness matrices is shown in Figs. 9-11. For the approximation order $p=2$ and for the new basis and the one by Zaglmayr [21], there are 76 versus 86 nonzero entries out of 144, accounting 52.78% versus 59.72%; and for $p=3$, 236 versus 272 out of 400, accounting 59.00% versus 68.00%; and for $p=4$, 532 versus 692 out of 900, accounting 59.11% versus 76.89%. Unlike the case with the mass matrices, now the stiffness matrices with both bases get denser with the increase of approximation order. However, with the new basis, the percentage of nonzero entries relative to the number of

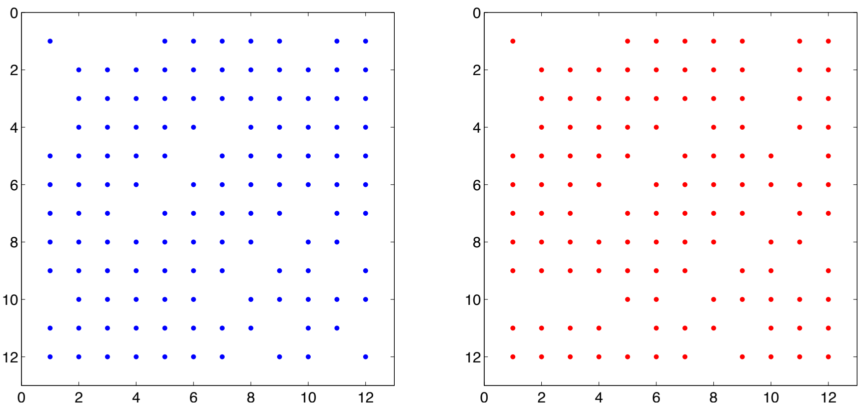

Figure 6: Sparsity of the mass matrix M_{p_2} for $\mathcal{H}(\mathbf{div})$-conforming triangular elements. Left: new basis, right: Zaglmayr basis [21].

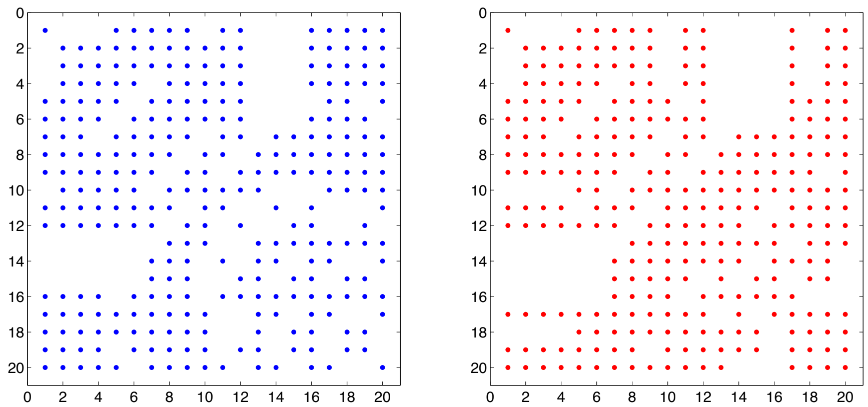

Figure 7: Sparsity of the mass matrix M_{p_3} for $\mathcal{H}(\mathbf{div})$-conforming triangular elements. Left: new basis, right: Zaglmayr basis [21].

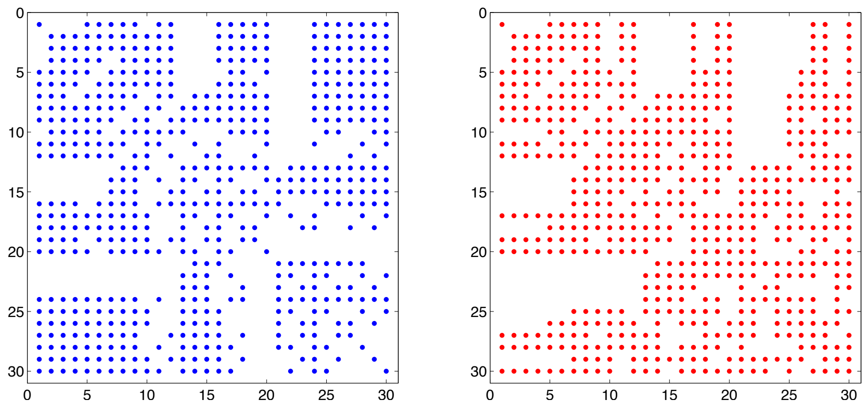

Figure 8: Sparsity of the mass matrix M_{p_4} for $\mathcal{H}(\mathbf{div})$-conforming triangular elements. Left: new basis, right: Zaglmayr basis [21].

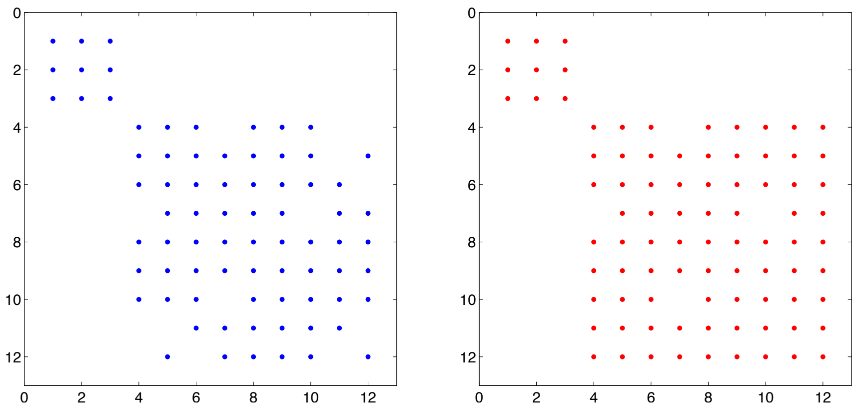

Figure 9: Sparsity of the stiffness matrix K_{p_2} for $\mathcal{H}(\mathbf{div})$-conforming triangular elements. Left: new basis, right: Zaglmayr basis [21].

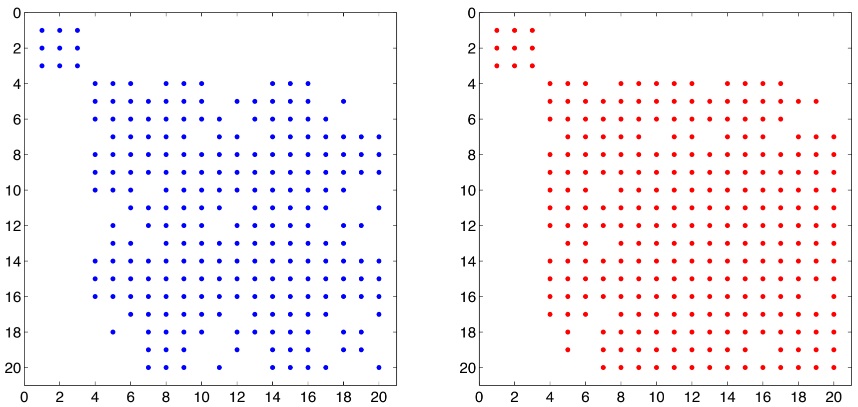

Figure 10: Sparsity of the stiffness matrix K_{p_3} for $\mathcal{H}(\mathbf{div})$-conforming triangular elements. Left: new basis, right: Zaglmayr basis [21].

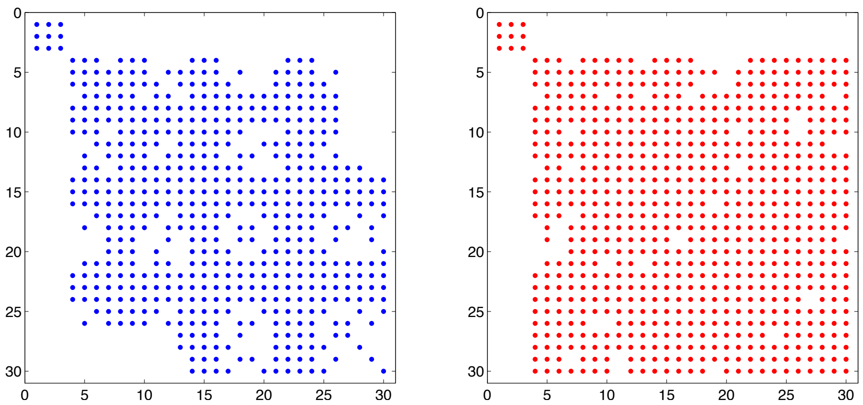

Figure 11: Sparsity of the stiffness matrix K_{p_4} for $\mathcal{H}(\mathbf{div})$-conforming triangular elements. Left: new basis, right: Zaglmayr basis [21].

the full matrix increases rather slowly. From Figs. 9-11 it can be seen that for each order of approximation, the stiffness matrix is much sparser with the new basis relative to the basis by Zaglmayr [21]. The most striking difference is with the approximation order four, for which the percentage of sparsity differs by more than 17%. Another observation is that with the new basis the stiffness matrix is relatively much sparser than the mass matrix for each order of approximation.

5 Discussion and conclusion

New hierarchical bases for simplicial $\mathcal{H}(\mathbf{div})$-conforming elements in two and three dimensions have been proposed with the goal of improving the conditioning of the mass and stiffness matrices. The construction of the new basis is motivated by the study of orthogonal polynomials of several variables [31] over an n-simplex. This is achieved by appropriately exploiting classical Jacobi polynomials over simplicial elements.

For the three-dimensional $\mathcal{H}(\mathbf{div})$-conforming tetrahedral elements, numerically it is found that for cubic polynomial approximation the condition numbers of the mass and stiffness matrices have grown up to order six, *i.e.* $\mathcal{O}(10^6)$. Thus, for the sake of reliability of numerical simulations, it is suggested that one may use the newly constructed hierarchical bases up to the third order but not beyond. The mass matrix is relatively sparser with the increase of approximation order. For a particular order of approximation, the mass matrix is even sparser than its corresponding two-dimensional one.

For the two-dimensional $\mathcal{H}(\mathbf{div})$-conforming triangular elements, it is identified numerically that for quadruple polynomial approximation the condition number of the mass matrix has increased up to order four, *i.e.* $\mathcal{O}(10^4)$. Therefore, to render numerical simulations being reliable, it is advised that one may use the newly constructed hierarchical bases up to the fourth order but not beyond. Up to fourth-order of approximation, the mass matrix from the new basis has better conditioning relative to the one from the Zaglmayr basis [21], the most significant improvement being the quadratic approximation. For the mass matrix and for the approximation up to order four, the newly derived basis has almost the same sparsity rate as the one by Zaglmayr [21]. Up to fourth-order of approximation, the stiffness matrix from the new basis is much sparser than that from the basis by Zaglmayr [21], and the percentage of sparsity differs by more than 17% for the fourth-order of approximation.

Acknowledgments

The first and second authors are supported in part by a DOE grant DEFG0205ER25678 and NSF grant DMS-1005441. The third author would like to thank Professor Joseph Coyle on the communication of the work presented in [18].

References

[1] F. Brezzi and M. Fortin, Mixed and Hybrid Finite Element Methods, Springer Series in Computational Mathematics, 15. Springer-Verlag, New York, 1991.

[2] J. E. Roberts and J.-M. Thomas, Mixed and Hybrid Methods, in Handbook of Numerical Analysis (Edited by P. G. Ciarlet and J.-L. Lions), Vol. II, pp. 523–639, North-Holland, Amsterdam, 1991.

[3] A. E. H. Love, A Treatise on the Mathematical Theory of Elasticity, 4th Ed., Dover Publication, New York, 1944.

[4] J. A. Stratton, Electromagnetic Theory, McGraw-Hill, New York, 1941.

[5] R. Temam, Navier-Stokes Equations: Theory and Numerical Analysis. With an appendix by F. Thomasset, 3rd Ed. Studies in Mathematics and Its Applications, 2. North-Holland Publishing, Amsterdam, 1984.

[6] T. G. Cowling, Magnetohydrodynamics, Interscience Tracts on Physics and Astronomy, No. 4. Interscience Publishers, New York, 1957.

[7] P. A. Raviart and J. M. Thomas, A mixed finite element method for 2nd order elliptic problems, Mathematical aspects of finite element methods (Proc. Conf. Consiglio Naz. delle Ricerche (C.N.R.), Rome, 1975), pp. 292–315. Lecture Notes in Math., Vol. 606, Springer, Berlin, 1977.

[8] J. C. Nédélec, Mixed finite elements in $\mathbb{R}^3$, Numer. Math., 35 (1980), pp. 315–341.

[9] J. C. Nédélec, A new family of mixed finite elements in $\mathbb{R}^3$, Numer. Math., 50 (1986), pp. 57–81.

[10] P. G. Ciarlet, Mathematical Elasticity Vol. I. Three-dimensional Elasticity. Studies in Mathematics and Its Applications, 20. North-Holland Publishing, Amsterdam, 1988.

[11] F. Brezzi, J. Douglas, Jr. and L. D. Marini, Two families of mixed finite elements for second order elliptic problems, Numer. Math., 47 (1985), pp. 217–235.

[12] F. Brezzi, J. Douglas, Jr., R. Durán and M. Fortin, Mixed finite elements for second order elliptic problems in three variables, Numer. Math., 51 (1987), pp. 237–250.

[13] R. Hiptmair, Canonical construction of finite elements, Math. Comp., 68 (1999), pp. 1325–1346.

[14] R. Hiptmair, Finite elements in computational electromagnetism, Acta Numer., 11 (2002), pp. 227–339.

[15] D. N. Arnold, R. S. Falk and R. Winther, Finite element exterior calculus, homological techniques, and applications, Acta Numer., 15 (2006), pp. 1–155.

[16] D. N. Arnold, R. S. Falk and R. Winther, Finite element exterior calculus: from Hodge theory to numerical stability, Bull. Amer. Math. Soc. (N.S.), 47 (2010), pp. 281–354.

[17] M. J. Bluck, Conforming hierarchical basis functions, Commun. Comput. Phys., 12 (2012), pp. 1215–1256.

[18] M. Ainsworth and J. Coyle, Hierarchic finite element bases on unstructured tetrahedral meshes, Internat. J. Numer. Methods Engrg., 58 (2003), pp. 2103–2130.

[19] J. E. Akin, Finite Elements for Analysis and Design, Academic Press, London, 1994.

[20] J. Xin, K. Pinchedez and J. E. Flaherty, Implementation of hierarchical bases in FEMLAB for simplicial elements, ACM Trans. Math. Software, 31 (2005), pp. 187–200.

[21] S. Zaglmayr, High Order Finite Element Methods for Electromagnetic Field Computation, Ph.D. Dissertation, Johannes Kepler Universität, Linz, 2006.

[22] I. Babuška, B. A. Szabo and I. N. Katz, The p-version of the finite element method, SIAM J. Numer. Anal., 18 (1981), pp. 515–545.

[23] I. Babuška and M. Suri, The p and $h-p$ versions of the finite element method, basic principles and properties, SIAM Rev., 36 (1994), pp. 578–632.
[24] P. Carnevali, R. B. Morris, Y. Tsuji and G. Taylor, New basis functions and computational procedures for p-version finite element analysis, Int. J. Num. Meth. Eng., 36 (1993), pp. 3759–3779.
[25] S. Adjerid, M. Aiffa and J. E. Flaherty, Hierarchical finite element bases for triangular and tetrahedral elements, Comput. Methods Appl. Mech. Engrg., 190 (2001), pp. 2925–2941.
[26] J. P. Webb, Hierarchal vector basis functions of arbitrary order for triangular and tetrahedral finite elements, IEEE Trans. Antennas and Propagation, 47 (1999), pp. 1244–1253.
[27] M. Ainsworth and J. Coyle, Hierarchic hp-edge element families for Maxwell's equations on hybrid quadrilateral/triangular meshes, Comput. Methods Appl. Mech. Engrg., 190 (2001), pp. 6709–6733.
[28] J. Xin and W. Cai, A well-conditioned hierarchical basis for triangular $\mathcal{H}(\mathbf{curl})$-conforming elements, Commun. Comput. Phys., 9 (2011), pp. 780–806.
[29] J. Xin, N. Guo and W. Cai, On the construction of well-conditioned hierarchical bases for tetrahedral $\mathcal{H}(\mathbf{curl})$-conforming Nédélec element, J. Comput. Math., 29 (2011), pp. 526–542.
[30] J. Xin and W. Cai, Well-conditioned orthonormal hierarchical $\mathcal{L}_2$ bases on $\mathbb{R}^n$ simplicial elements, J. Sci. Comput., 50 (2012), pp. 446–461.
[31] C. F. Dunkl and Y. Xu, Orthogonal Polynomials of Several Variables, Encyclopedia of Mathematics and its Applications, 81. Cambridge University Press, Cambridge, 2001.
[32] W. Magnus, F. Oberhettinger and R. P. Soni, Formulas and Theorems for the Special Functions of Mathematical Physics, Die Grundlehren der mathematischen Wissenschaften, Band 52, Springer-Verlag, New York, 3rd enlarged edition, 1966.
[33] R. Dautray and J.-L. Lions, Mathematical Analysis and Numerical Methods for Science and Technology, Vol. 3. Spectral Theory and Applications, Springer-Verlag, Berlin, 1990.
[34] O. D. Kellogg, Foundations of Potential Theory, Reprint from the first edition of 1929. Die Grundlehren der Mathematischen Wissenschaften, Band 31, Springer-Verlag, New York, 1967.
[35] B. Cockburn, G. Kanschat and D. Schötzau, A note on discontinuous Galerkin divergence-free solutions for the Navier-Stokes equations, J. Sci. Comput., 31 (2007), pp. 61–73.
[36] C. Greif, D. Li, D. Schötzau and X. Wei, A mixed finite element method with exactly divergence-free velocities for incompressible magnetohydrodynamics, Comput. Methods Appl. Mech. Engrg., 199 (2010), pp. 2840–2855.